Earth and Planetary Science Letters 461 (2017) 151–162

Contents lists available at ScienceDirect

Earth and Planetary Science Letters

www.elsevier.com/locate/epsl

Timing, duration, and causes for Late Jurassic–Early Cretaceous anoxia in the Barents Sea

Svetoslav V. Georgiev [a,*], Holly J. Stein [a,b], Judith L. Hannah [a,b], Guangping Xu [a], Bernard Bingen [c], Hermann M. Weiss [d,1]

[a] AIRIE Program, Colorado State University, Fort Collins, 80523-1482 CO, USA
[b] Centre for Earth Evolution and Dynamics, University of Oslo, 0316 Oslo, Norway
[c] Geological Survey of Norway, 7491 Trondheim, Norway
[d] SINTEF Petroleum Research, 7465 Trondheim, Norway

ARTICLE INFO

Article history:
Received 16 June 2016
Received in revised form 16 December 2016
Accepted 25 December 2016
Available online 13 January 2017
Editor: M. Frank

Keywords:
Re–Os
geochronology
shale
redox
time scale
Hekkingen Formation

ABSTRACT

Re–Os isochron ages for black shales of the Hekkingen Formation in the Barents Sea constrain the onset (157.7 ± 1.3 Ma) and termination (138.8 ± 1.0 Ma), and thereby indicate a long duration (~19 Myr) of widespread Jurassic–Cretaceous anoxia in the Arctic. Integration of these new Re–Os ages with published radiometric ages, ammonite biostratigraphy and geomagnetic polarity chrons shows shorter late Oxfordian–late Kimmeridgian and longer Berriasian stages relative to estimates in the 2012 and 2016 Geological Time Scales. Late Jurassic anoxia was likely the result of warming climate due to high atmospheric CO_2 levels from increased oceanic crust production. Rising temperatures enhanced weathering and nutrient supply, increased productivity, and slowed ocean circulation before a sea-level rise brought anoxic waters onto continental shelves. Assessment of new and published Os- and Sr-isotopic data suggests that prolonged oceanic anoxia required a sustained CO_2 source from fast spreading rates and/or longer subduction zones and spreading ridges to balance large burial of carbon in voluminous Upper Jurassic and Lower Cretaceous black shales.

1. Introduction

Late Jurassic–Early Cretaceous time was marked by widespread anoxia in epicontinental and deep basins, particularly in the circum-Arctic region (e.g., Leith et al., 1993; Gröcke et al., 2003; Pearce et al., 2010), and perhaps in parts of the deep ocean (Nozaki et al., 2013). Anoxic waters favored the deposition and preservation of organic-rich sediments (black shales) with excellent oil-generating capacity, especially in northern latitudes (e.g., Klemme and Ulmishek, 1991; Leith et al., 1993). Causes for this widespread anoxia are still debated. The most widespread and voluminous black shale deposition in the Arctic started during the late Oxfordian and in most localities persisted until the Berriasian–Valanginian (Leith et al., 1993). Widespread anoxia in northern latitudes occurred during a long period of overall warm climate (e.g., Price and Rogov, 2009), high atmospheric CO_2 concentrations (3 to 5 times present-day; Berner and Kothavala, 2001) and increased continental weathering (e.g., Gröcke et al., 2003). Anoxic conditions developed a few million years after cool temperatures and presumed glaciation near the Callovian–Oxfordian boundary (Dromart et al., 2003), at a time of significant stepwise climate warming, rapid weakening of equatorial upwelling and waning of shelf currents (Rais et al., 2007) and remarkably low seawater $^{87}Sr/^{86}Sr$ values (e.g., Jones and Jenkyns, 2001; McArthur et al., 2012). This drop in Sr isotopic ratios during a period of climate warming (e.g., Dera et al., 2011) and sea-level rise, which should raise seawater $^{87}Sr/^{86}Sr$ through increased chemical weathering of continents, likely reflects intense mid-ocean ridge hydrothermal activity (Jones and Jenkyns, 2001) also recorded in increasing manganese supply to seawater (Corbin et al., 2000). Another interesting feature of the Late Jurassic is prolonged and massive drawdown of carbon in black shales, as evidenced by the widespread occurrence of organic-rich sediments (e.g. Leith et al., 1993). Normally, this would lower atmospheric CO_2, causing climate cooling and termination of anoxia, as oxygen solubility in seawater is reversely correlated with temperature. Instead, sustained black shale deposition in overall warming climates prevailed with possible cooling only in the Berriasian (e.g., Price et al., 2016, and references therein). Initial $^{187}Os/^{188}Os$ ratios (Os_i) of organic-rich shale provides a tool for reconstructing Earth's geo-

* Corresponding author.
E-mail address: georgiev@colostate.edu (S.V. Georgiev).
[1] Deceased.

http://dx.doi.org/10.1016/j.epsl.2016.12.035
0012-821X/

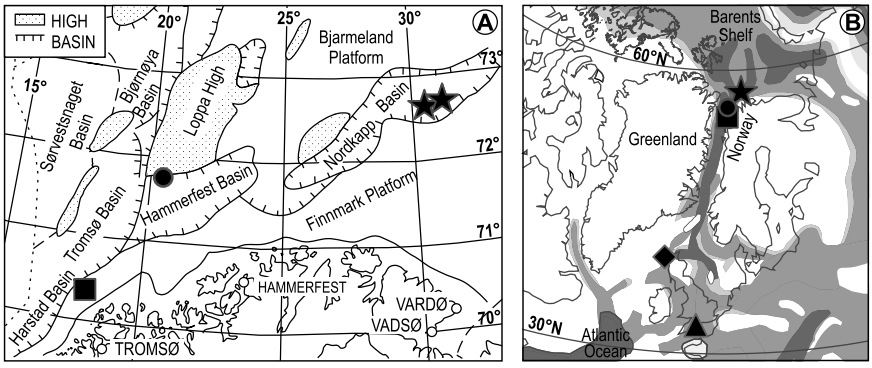

Fig. 1. A) Location of studied cores from the Nordkapp Basin (stars; cores 7231/01-U-01 and 7230/05-U-02) and from the Troms III area at the NE margin of the Harstad Basin (square; core 7018/05-U-01), and published core with Re–Os data from the Skalle prospect in the Hammerfest Basin (circle; Markey et al., 2017) in the Barents Sea region (map after Gabrielsen et al., 1990); B) Late Jurassic paleogeographic reconstruction, Greenland–Norway seaway region, outlining areas for deposition of deltaic to deep marine sediments (pale gray to dark gray; modified after Torsvik et al., 2002). New Re–Os data from the Nordkapp Basin and Troms III, and published Re–Os data from Hammerfest Basin (circle; Markey et al., 2017), Kimmeridge Clay (triangle; Cohen et al., 1999) and Isle of Skye (diamond; Selby, 2007) are plotted relative to the reconstructed Late Jurassic paleo-shoreline.

chemical cycles and determining causes for Late Jurassic anoxia in the Barents Sea. This is because Os_i usually reflects the $^{187}Os/^{188}Os$ of contemporaneous seawater (e.g., Ravizza and Turekian, 1992; Cohen et al., 1999; Georgiev et al., 2011), which in turn tracks the balance between Os supply from continental runoff (presently with high $^{187}Os/^{188}Os > 1$) and mantle or cosmic dust (low $^{187}Os/^{188}Os$ at ~0.13) (e.g., Peucker-Ehrenbrink and Ravizza, 2000).

Knowledge of the extent and causes of this widespread marine anoxia across the Arctic depends on refined temporal correlations of lithostratigraphy. However, the earliest Cretaceous and especially the Late Jurassic lack precise radiometric ages for narrow, well-defined biostratigraphic intervals (e.g., Pálfy, 2008; Gradstein et al., 2012), mainly because marine sediments from that time often lack volcanic horizons suitable for U–Pb or $^{40}Ar/^{39}Ar$ dating. Black shales, however, are typically well-suited for Re–Os geochronology (e.g., Kendall et al., 2009; Georgiev et al., 2011). Two Late Jurassic Re–Os shale ages (Cohen et al., 1999; Selby, 2007) are included in the latest full Geological Time Scale (GTS2012; Gradstein et al., 2012) as secondary guides, but they are not used for calculation of stage boundaries. Instead, ages for the Bajocian to Barremian stages are derived almost exclusively by: 1) computing the duration of ammonite zones from cyclostratigraphy; 2) calibrating to a spreading rate model for the M-sequence (Mesozoic) marine magnetic anomalies; and 3) calibrating this spreading rate to selected numerical ages (GTS2012, p. 736). A similar model is used in the concise Geological Time Scale 2016 (GTS2016, Ogg et al., 2016). Importantly, the GTS2012 model for decreasing spreading rates from the Bajocian to Barremian stages is anchored by only two radiometric ages spanning ~82 Myr: the base of the Cenomanian (100.5 ± 0.4 Ma) and the base of the Toarcian (182.7 ± 0.7 Ma). This presents a challenge for the Late Jurassic–Early Cretaceous time scale, because in essence a floating cyclostratigraphy for that interval is time-anchored by calibration to a spreading rate model that is also based on the same floating cyclostratigraphy. The few available radiometric ages match relatively well with GTS2012 earliest Cretaceous stage boundaries, but the few available precise Late Jurassic Re–Os and $^{40}Ar/^{39}Ar$ ages tied to biostratigraphy (Selby, 2007; Pellenard et al., 2013) are younger than indicated by GST2012 or GTS2016 and agree better with GTS2004 (Gradstein et al., 2004).

Here we present precise Re–Os depositional isochron ages for organic-rich, biostratigraphically-dated shales from the Barents Sea. Using ages and isochron-derived initial $^{187}Os/^{188}Os$ ratios, regional and global correlations help address the duration and causes for widespread anoxia in the Late Jurassic–Early Cretaceous.

2. Geological setting and studied material

The Barents Shelf consists of deep basins and prominent highs between mainland Norway and Svalbard (e.g., Gabrielsen et al., 1990). Rift-related subsidence and a major sea-level rise near the onset of the Late Jurassic initiated widespread deposition of marine black shales of the Hekkingen Formation (Dalland et al., 1988; Leith et al., 1993; Torsvik et al., 2002), broadly correlative with prolific source rocks from southern England (Kimmeridge Clay) and on the Norwegian shelf (e.g., Leith et al., 1993; Mutterlose et al., 2003; Fig. 1).

We sampled organic-rich shale of the Hekkingen Formation from three offshore wells in the Troms III (Smelror et al., 2001) and the Nordkapp Basin (Bugge et al., 2002) areas. The Troms III drill hole IKU 7018/05-U-01 (coordinates 70°30′18.18″N and 18°22′28.22″W) lies near the NE margin of the Harstad Basin between the Barents and Norwegian Seas (Smelror et al., 2001) (Fig. 1). The Nordkapp Basin is a 300-km-long, NE-trending feature in the SW Barents Sea, occupying a deep marine Triassic–Jurassic embayment (Gabrielsen et al., 1990; Bugge et al., 2002) (Fig. 1). Here, we sampled IKU drill core 7230/05-U-02 (coordinates 72°40′51.1″N and 30°22′29.51″W) and IKU drill core 7231/01-U-01 (coordinates 72°45′12.45″N and 31°7′30.21″W) (Bugge et al., 2002). Late Jurassic–Early Cretaceous paleolatitudes were ~50°–55°N for Troms III and ~53°–58°N for the Nordkapp Basin based on reconstructions by Mutterlose et al. (2003) and Torsvik et al. (2002).

Regionally, Middle Oxfordian strata are absent over much of the Barents Sea, including the two studied sites (Smelror et al., 2001). Laminated, organic-rich (~2–26 wt% total organic carbon, TOC) shales of the Hekkingen Formation overlie this regional unconformity. These shales were deposited between the Late Oxfordian and the Boreal Berriasian in Troms III (Smelror et al., 2001) and up until the Early Volgian (early-mid Tithonian) in the Nordkapp Basin (Bugge et al., 2002). The Hekkingen Formation is subdivided into a lower Alge Member with characteristically high gamma-ray readings and high TOC, and an upper Krill Member with lower TOC contents and lower gamma-ray readings (Dalland et al., 1988). This subdivision is readily applicable to the Troms III section (Smelror et al., 2001), but it is less clear for the Nordkapp Basin section where both Alge and Krill shales have similarly high TOC contents (Fig. 2) and a more homogeneous gamma-ray signal (data of Bugge et al., 2002). At both sites, the Hekkingen Formation is sharply overlain by lower Valanginian–Hauterivian claystone and limestone of the condensed Klippfisk Formation.